

## Fatigue behavior of concrete beams reinforced with HRBF500 steel bars

Ke Li<sup>1a</sup>, Xin-Ling Wang<sup>2b</sup>, Shuang-Yin Cao<sup>\*1</sup> and Qing-Ping Chen<sup>3</sup>

<sup>1</sup>Department of Civil Engineering, Key Laboratory of Concrete and Prestressed Concrete Structures of the Ministry of Education, Southeast University, Nanjing 210096, P.R. China

<sup>2</sup>Department of Civil Engineering, Zhengzhou University, Zhengzhou 450002, P.R. China

<sup>3</sup>Department of Civil Engineering, Kaifeng University, Kaifeng 475000, P.R. China

(Received May 4, 2013, Revised May 6, 2014, Accepted June 9, 2014)

**Abstract.** The purpose of this study was to investigate experimentally the fatigue performance of reinforced concrete (RC) beams with hot-rolled ribbed fine-grained steel bars of yielding strength 500MPa (HRBF500). Three rectangular and three T-section RC beams with HRBF500 bars were constructed and tested under static and constant-amplitude cyclic loading. Prior to the application of repeated loading, all beams were initially cracked under static loading. The major test variables were the steel ratio, cross-sectional shape and stress range. The stress evolution of HRBF500 bars, the information about crack growth and the deflection developments of test beams were presented and analyzed. Rapid increases in deflections and tension steel stress occurred in the early stages of fatigue loading, and were followed by a relatively stable period. Test results indicate that, the concrete beams reinforced with appropriate amount of HRBF500 bars can survive 2.5 million cycles of constant-amplitude cyclic loading with no apparent signs of damage, on condition that the initial extreme tensile stress in HRBF500 steel bars was controlled less than 150 MPa. It was also found that, the initial extreme tension steel stress, stress range, and steel ratio were the main factors that affected the fatigue properties of RC beams with HRBF500 bars, whose effects on fatigue properties were fully discussed in this paper, while the cross-sectional shape had no significant influence in fatigue properties. The results provide important guidance for the fatigue design of concrete beams reinforced with HRBF500 steel bars.

**Keywords:** HRBF500 steel bar; fatigue performance; RC beam; constant-amplitude cyclic loading

### 1. Introduction

HRBF500 steel bar is a successfully developed new-type steel in China. HRBF500 bars are produced by using a thermo mechanically controlled process. As a new generation of steel materials, very fine grained metallic material with a grain measured in micrometers or less have aroused sustaining interest in recent years because of their excellent physical and mechanical properties, such as high strength as well as fairly good ductility, formability, superplasticity, etc

---

\*Corresponding author, Professor, E-mail: 101000873@seu.edu.cn

<sup>a</sup>Ph.D. Student

<sup>b</sup>Professor

(Park *et al.* 2000, Takaki *et al.* 2001). In order to promote the application of fine-grained steels in practical engineering, plenty of experimental verifications need to be done. The fatigue behavior research of reinforced concrete structures reinforced with fine-grained steels ought to be an important aspect, because concrete structures are widely used, and many of them are subjected to cyclic loads such as main girders of bridges, reinforced concrete pavements, crane girders, offshore platforms and so forth.

Fatigue properties of RC structures depend on the performance of their components. Fatigue loading causes progressive deterioration of bond between reinforcement and concrete, and produces a time-dependent redistribution of the stresses, which lead to a drop in concrete tensile stresses and a mild increase in steel stresses (Al-Rousan and Issa 2011, El-Tawil *et al.* 2000). Larger crack widths and a smaller contribution of concrete in tension between the cracks result in larger deflection (Shahawy and Beitelman 1999). The fatigue behavior of RC beams is mostly controlled by the fatigue behavior of the reinforcing steel (Aidoo and Harries 2004). Fatigue failure of RC beams is caused generally by successive fracturing of the reinforcement (Muller and Dux 1994, Grace and Ross 1996). Another failure mechanism is spalling of concrete in the compression zone. However, even over-reinforced beams (i.e. concrete compression failure under static loading) fail due to reinforcement fracture when subjected to fatigue loading. Findings from past investigations focusing on fatigue endurance of concrete beams have indicated that beam performance can be influenced by a number of different parameters. These parameters include the design tensile stress limit, stress range, steel ratio, status of the bottom concrete (cracked or uncracked), and variations in beam section properties (Kormeling 1980, Kennedy *et al.* 1990). The risk of fatigue failure in cracked concrete beams is greater than uncracked ones (Roller *et al.* 2007). Increasing stress ranges of steel reinforcements in RC beams may result in more reduction in static loading capacity, stiffness and fatigue life of the beams (Al-Hammoud *et al.* 2010, Heffernan and Erki 2004, Kim and Harries 2011).

Similar experimental studies on the fatigue performance of reinforced concrete beams have been carried out by researchers. Thandavamoorthy (1999) conducted experimental investigations on the concrete beams reinforced with high-ductility bars (steel ribbed bars with low carbon content and higher ductility, having different chemical composition and mechanical properties, and produced by a different manufacturing technique called the tempcore process). In this study, eight beams were tested in fatigue (Four beams were tested under three-point bending and a further four by four-point bending). Test results indicate that deflection, crack width, and average curvature of tested beams at maximum load limit increase with the number of cycles, as has been observed earlier in the context of concrete beams reinforced with conventional steel. In addition, the mode of loading also influences the fatigue behavior of beams. For instance, the increase in deflection and curvature of beams tested under three-point bending are greater than that of beams tested under four-point bending, while the increase in the measured maximum crack width at the level of tension reinforcement was greater for beams tested under four-point bending than for those under three-point bending. Shahawi *et al.* (1986) conducted experimental investigations on the fatigue behavior of partially prestressed concrete beams. In this study, eight beams were tested in fatigue (five beams are subjected to a constant load cycle, while the remaining three beams are subjected to cumulative fatigue loading). In this test, pronounced increases in deflection, crack widths and nonprestressed steel stress occurred in the early stages of testing, after which a stable period of behavior was observed. It was found that a degree of prestress between 0.4 and 0.6 is optimum for satisfactory cracking and fatigue response.

Besides, there have been a limited number of experimental studies on the fatigue behavior of

ultrafine-grained steels. In general, the fatigue strength of ultrafine-grained steels is enhanced considerably by grain refinement, in particular in the high cycle fatigue regime (Chapetti *et al.* 2004, Okayasu *et al.* 2008, Mughrabi and Höppel 2010). However, at the same time, the low cycle fatigue performance is impaired by microstructural instabilities of the strongly hardened but less ductile ultrafine-grained materials (Patlan *et al.* 2001). Fatigue crack growth resistance and the threshold of ultrafine grained steel were lower than that of an as-received coarse grained steel (Chapetti *et al.* 2005, Kim *et al.* 2003).

However, so far, no information is available on fatigue performance of RC structures with fine-grained steel reinforcements. At present, HRBF500 steel bars are available by being massively produced and to be applied to high-speed railway viaducts because of their low-cost, high-strength and many other advantages (Park *et al.* 2000, Takaki *et al.* 2001). Since a new material, different from the conventional steel, is available for reinforcing concrete, there is a greater need to study its suitability as steel reinforcement and also its behavior under cyclic loadings.

In this paper, the fatigue performances of HRBF500 bars RC beams were investigated. Three rectangular and three T-section HRBF500 bars RC beams of different steel ratios and were designed and tested under constant amplitude cyclic load. The general aims of the research reported in this paper were: (1) to examine the fatigue behavior of HRBF500 steel bars in RC beams operating in a cracked condition; (2) to explore the main factors affecting the fatigue performance of HRBF500 bars RC beams and how these factors function; (3) to determine maximum allowable extreme reinforcement tensile stress in HRBF500 bars RC beams under fatigue loading.

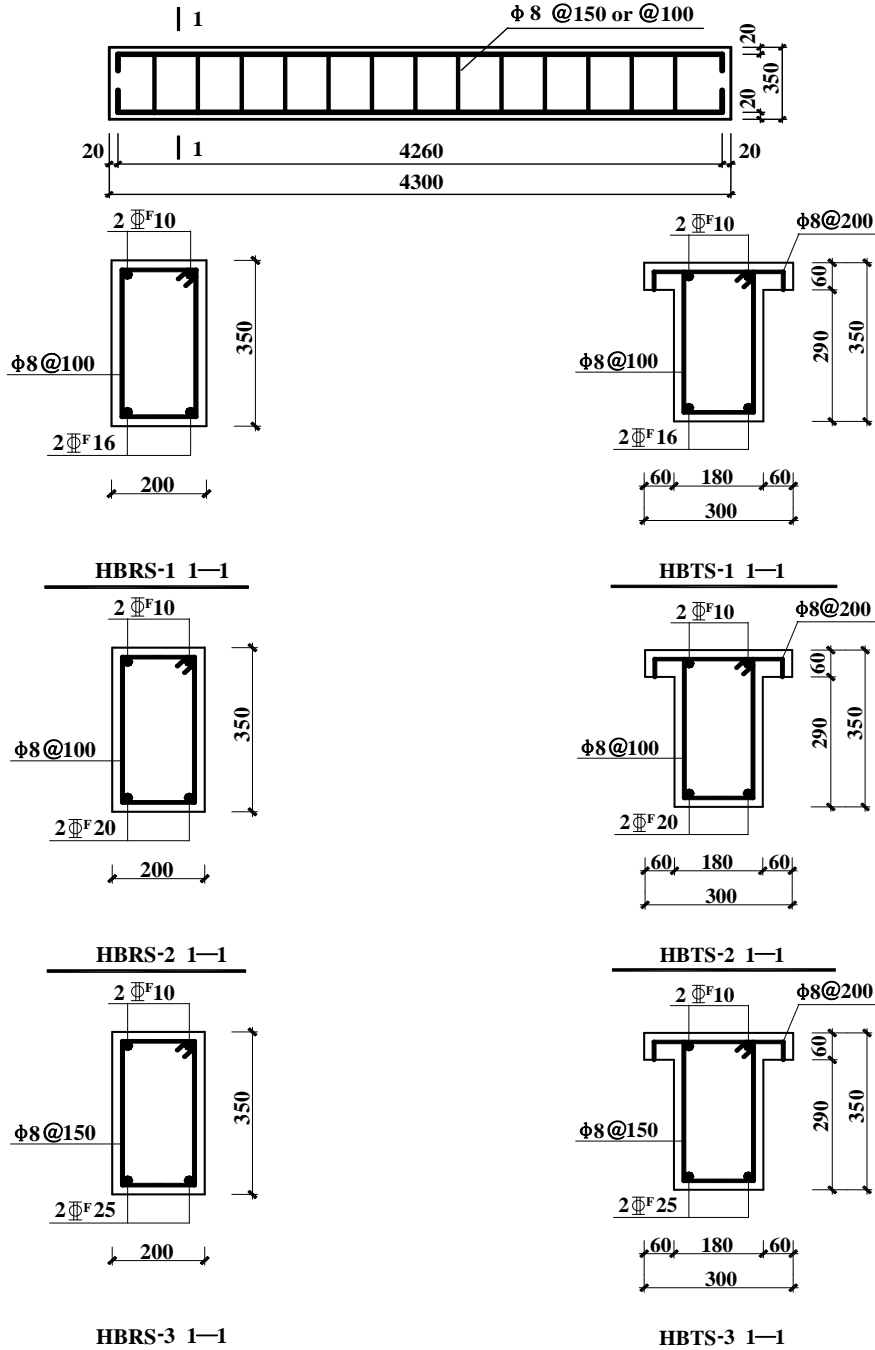
## 2. Experimental program

### 2.1 Design of test beams

Three rectangular and three T-section RC beams were designed according to the Chinese Standard Code for Design of Reinforced Concrete and Prestressed Concrete Structures used in Railways and Bridges TB10002.3-2005. The beams were designed with varying values of steel ratios. The three rectangular RC beams having the same overall dimensions were represented by HBRS-1, HBRS-2 and HBRS-3, respectively. And the further three T-section RC beams having the same overall dimensions were respectively represented by HBTS-1, HBTS-2 and HBTS-3. The geometric dimensions and reinforcement details of the test beams are shown in Fig. 1.

### 2.2 Material properties

Longitudinal reinforcements of the test beams were ultra-fine grained steels with characteristic value yielding strength 500 MPa (HRBF500). The HRBF500 steel bars used in the specimens were tested in the laboratory and the mechanical properties were shown in Table 1. The concrete of all the test beams was commercial concrete designed with a C50 grade of compressive strength, according to the Chinese Standard Code for Design of Concrete Structures GB50010-2002. Ten 150 mm×150 mm×150 mm concrete cube specimens were made at the same time of casting of the test beams and were cured with the same way as the beams, and then the average 28-day concrete cube strength and elasticity modulus was tested. The axial compressive strength was 64 MPa and the elasticity modulus was 37600 N/mm<sup>2</sup>.



Note: This symbol  $\Phi^F$  stands for HRBF500 bars and  $\Phi$  for hot-rolled plain-shaped bars with yielding strength 235 Mpa (HPB235); the numbers before  $\Phi^F$  or  $\Phi$  indicate the amount of steel bars and the numbers followed mean for the diameter of steel bars in mm, i.e.,  $2\Phi^F10$  means two 10-mm-diameter HRBF500 steel bars. The numbers following “@” represent the spacing between steel bars in mm, i.e.,  $\Phi8@150$  means 8-mm-diameter HPB235 steel bars with spacing of 150 mm.

Fig. 1 Section dimensions and reinforcement details of specimens

Table 1 The mechanical properties of HRBF500 bars

Bar diameter (mm)	10 mm	16 mm	20 mm	25 mm
Ultimate elongation strain (%)	18%	26.56%	23%	25.2%
Yielding strength (N/mm <sup>2</sup> )	540	515	494	531.5
Ultimate tensile strength (N/mm <sup>2</sup> )	697	659	656	687
Elasticity modulus (N/mm <sup>2</sup> )	$1.95 \times 10^5$	$1.94 \times 10^5$	$2.07 \times 10^5$	$2.03 \times 10^5$

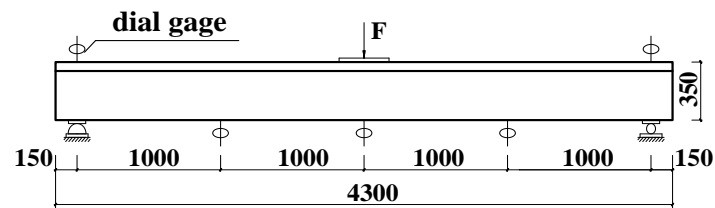


Fig. 2 Loading schemes and placement of displacement transducers



Fig. 3 Details of the setup of fatigue test

### 2.3 Test setup and procedure

In the fatigue test, the test beams were simply supported near the ends creating a total span length of 4000 mm, and loaded repeatedly at the mid-span (Fig. 2). Fig. 3 is a photograph of the fatigue loading test setup. Arrangement of measuring points in the test beams was as follows: electrical resistance strain gauges were adhered to longitudinal steel bars at the mid-span and stirrups of test beams to measure the tensile strain of steel reinforcements. Fig. 2 shows the placement of displacement transducers dial gages used for measuring the deflections of test beams.

The upper-bound fatigue load was defined to provide the maximum stress of greater than 150 Mpa in the HRBF500 tension steels to simulate the limit stress state of HRBF500 bars used in high-speed railway viaducts under dynamic load. Each test beam was cracked prior to application of fatigue loading. This was achieved by subjecting the specimen to a static loading up to the load that produced tensile stress of more than 150 MPa in HRBF500 bars. Cracks were marked, and the test beam was then unloaded. The specimen was reloaded in increments up to the previous

Table 2 Loading program of fatigue test

Specimen no.	The upper-bound fatigue load (kN)	The lower-bound fatigue load (kN)	Initial minimum stress	Initial maximum stress (MPa)	Frequency (HZ)
HBTS-1	20	16	$0.03f_y^*$	152.91	4
HBTS-2	23	18	$0.03f_y^*$	154.37	4
HBTS-3	46	24.4	$0.03f_y^*$	152.05	4
HBTS-1	28.5	14.5	$0.03f_y^*$	162.86	4
HBTS-2	20.2	11	$0.03f_y^*$	155.31	4
HBTS-3	50.8	25	$0.03f_y^*$	153.32	4

$f_y^*$ : yield strength of HRBF500 steel .

maximum load level, and readings of strain and deflection were recorded at each load increment. Then, the six beams were subjected to constant-amplitude cyclic loading by using a dynamic hydraulic jack for 2.5 million cycles. The upper-bound and lower-bound fatigue load, the initial maximum and minimum stress of tension reinforcement at first cycle, and loading frequency were specified in Table 2. The frequency and amplitude of applied fatigue load were controlled and measured by closed-loop servo-hydraulic fatigue testing system. When the load cycles reached 10,000, 100,000, 500,000, 1 million, 1.5 million, 2 million and 2.5 million times, the test was stopped and a static loading test with loading increased from 0 to the upper-bound fatigue load was done, measuring strain, deflection and crack width of the test beams.

### 3. Test results and discussion

#### 3.1 Cracks development

For specimen HBRS-1, HBRS-2, HBRS-3, HBTS-2 and HBTS-3, new vertical cracks appeared near the mid-span intermittently with increasing number of load cycles, with cracks widths increased gradually. When loading cycles increased to approximately 100,000, existing cracks produced by static loading of the above five test beams began to extend gradually toward the top of the beams. The change in maximum cracks widths with increasing number of load cycles for specimen HBRS-1, HBRS-2, HBRS-3, HBTS-2 and HBTS-3 were shown in Table 3. As Table 3 shows, the maximum widths of cracks increased discontinuously, and were not more than 0.2 mm after 2.5 million loading cycles. In addition, there are no significant differences in evolution law of maximum cracks widths between rectangular and T-section beams.

For specimen HBTS-1, when loading cycles increased to 100,000, the maximum width of cracks reached 0.1 mm, and when loading cycles increased to 320,000, the maximum width of cracks near the mid-span increased to 1 mm suddenly, with the crack extending up to the top of the beams, and at the same time the tensile reinforcement stress suddenly increased to the yielding strength, which indicated the impending occurrence of brittle failure of specimen HBTS-1, and then the test was stopped. As Table 2 shows, only the initial tensile stress of HRBF500 bars of specimen HBTS-1 reached more than 160 MPa, the other specimens' were just a little more than 150 MPa. This indicated that, on condition that the initial tensile stress of HRBF500 reinforcement bars produced by the upper-bound fatigue load were not more than 150 Mpa, the RC beams with

Table 3 The maximum crack width of four specimens at different fatigue cycles  $N$  (unit: mm)

specimen no.	$N$							
	10000	100000	500000	1 million	1.5 million	2 million	2.5 million	
HBRS-1	0.1	0.1	0.1	0.1	0.1	0.2	0.2	
HBRS-2	0.05	0.05	0.05	0.1	0.1	0.1	0.1	
HBRS-3	0.1	0.1	0.2	0.2	0.2	0.2	0.2	
HBTS-2	0.05	0.1	0.1	0.1	0.1	0.1	0.1	
HBTS-3	0.1	0.15	0.15	0.2	0.2	0.2	0.2	

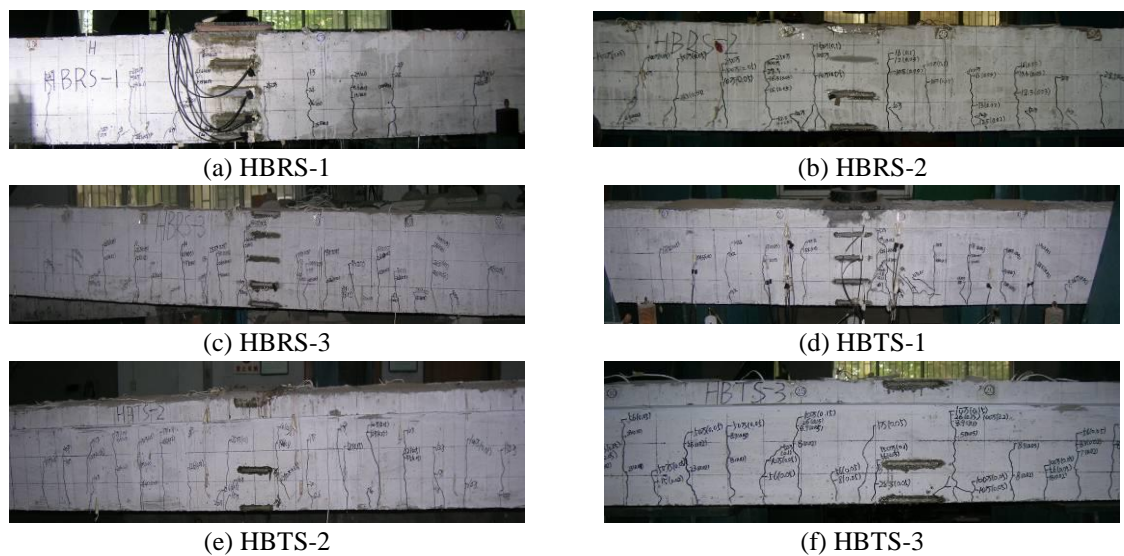


Fig. 4 Cracks of specimens after fatigue test

HRBF500 reinforcement bars could withstand 2.5 million cycles of fatigue loading under the load level listed in Table 3, and presented good fatigue resistance. The crack distribution of the six test beams after 2.5 million cycles of loading was presented in Fig. 4.

### 3.2 Deflections analysis

Fig. 5 shows the relationship between the number of load cycles and the mid-span deflections under maximum fatigue load for specimens. As Fig. 5 shows, there was pronounced increases in mid-span deflections in the initial 100,000 cycles, after which stable behaviors were observed with only slight increases in mid-span deflections. In addition, there are no significant differences in evolution law of mid-span deflections for rectangular and T-section beams. The percentage increase in deflection over the initial value for each beam is given in Table 4. As Table 4 shows, of those specimens except specimen HBTS-1, the bigger the steel ratio was, the smaller the percentage increase in mid-span deflection was. The rate of mid-span deflection increase for specimen HBTS-1 was fastest of all because the initial tensile stress of HRBF500 bars in specimen HBTS-1 produced by the upper-bound fatigue loads was biggest.

As discussed above, number of load cycles  $N$ , steel ratio and the initial tensile stresses of

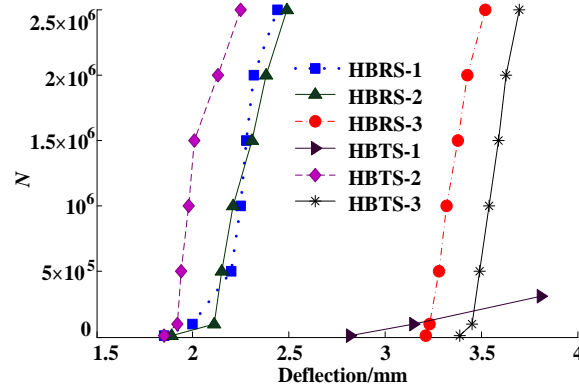
Fig. 5 The number of load cycles  $N$  versus mid-span deflection

Table 4 The percentage increase in deflection and tension steel strain

Specimen no.	Tensile reinforcement ratio $\rho$ (%)	Number of cycles (millions)	Percentage increase over initial values	
			Deflection	Tension steel strain
HBTS-1	0.5743	2.5	44.9	79.4
HBTS-2	0.8971	2.5	41.5	43.2
HBTS-3	1.4029	2.5	19.7	17.8
HBTS-1	0.6380	0.32	40.6	264
HBTS-2	0.9968	2.5	35.5	35.1
HBTS-3	1.5587	2.5	13.5	16.9

HRBF500 bars were the main factors affecting the deflection increase. Then the quantitative relationship between the deflection increase and number of load cycles  $N$  was analyzed in the stable growth stage (number of load cycles  $N$  was not less than 10,000) for the test beams that survived 2.5 million cycles of constant-amplitude cyclic loading, as well as the relationship between the deflection increase and steel ratio.

Deflection increase coefficient  $\kappa$  was defined as follow

$$\kappa = f / f_1 - 1 \quad (1)$$

where  $f_1$  denotes the mid-span deflection of specimens corresponding to the maximum fatigue load in the static load test before the fatigue test; and  $f$  represents the mid-span deflection of specimens corresponding to the maximum fatigue load at different load cycles in fatigue test.

According to experimental data, the relationship between deflection increase coefficient  $\kappa$  and the number of number of load cycles for specimen HBRS-1 is shown in Fig. 6. As indicated in Fig. 6, deflection increase coefficient  $\kappa$  increased linearly with increasing number of load cycles  $N$ . Through linear regression, the relationship between increase coefficient  $\kappa$  and number of load cycles  $N$  was expressed as follow:

$$\kappa = 0.001n + 0.2279 \quad (2)$$

where  $n=10^{-4} N$ .

Similarly, the relationship between increase coefficient  $\kappa$  and number of load cycles  $N$  for the

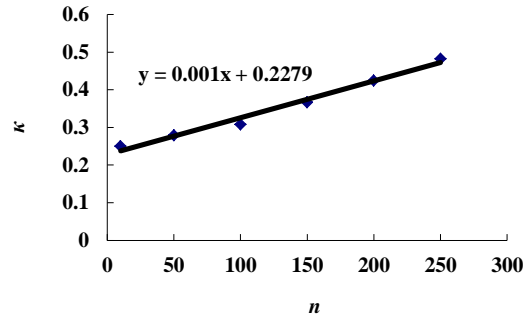


Fig. 6 The deflection increase coefficient  $\kappa$  versus  $n$

other 4 specimens were obtained as follow

$$\text{specimen HBRS-2: } \kappa = 0.0009n + 0.1784 \tag{3}$$

$$\text{specimen HBRS-3: } \kappa = 0.0004n + 0.0925 \tag{4}$$

$$\text{specimen HBTS-2: } \kappa = 0.0008n + 0.1263 \tag{5}$$

$$\text{specimen HBRS-3: } \kappa = 0.0003n + 0.0547 \tag{6}$$

The mean value of the ratio of calculated values according to Eqs. (2)-(6) to experimental values was 0.9963, and the standard deviation and coefficient of variation were 0.0729 and 0.073 respectively, which indicated that the calculated values consisted well with experimental results. Through analysis of the Eqs. (2)-(6), it can be found that, relationship between deflection increase coefficient  $\kappa$  and number of load cycles  $N$  for the test beams can be expressed by the equation as follows

$$\kappa = an + b \tag{7}$$

Then the influence of tension reinforcement ratio in the coefficient  $a$  and  $b$  in Eq. (7) was mainly considered. By linear regression, the relationship between the coefficient  $a$  and  $b$  in Eqs. (2)-(6) and tension reinforcement ratio  $\rho$  can be expressed as

$$a = -0.0926\rho + 0.0017 \tag{8}$$

$$b = -18.276\rho + 0.3436 \tag{9}$$

Taking Eqs. (1), (8) and (9) into Eq. (7), the values of mid-span deflections under maximum fatigue load can be calculated from the following expressions

$$f = [(-0.0926\rho + 0.0017)n - 18.276\rho + 0.3436 + 1]f_1 \tag{10}$$

where tension reinforcement ratio  $\rho$  is given by

$$\rho = A_s / bh \tag{11}$$

where  $A_s$  is tension reinforcement area,  $h$  is the depth of the beam section,  $b$  is the width of the section for rectangular beam or the web for T-section beam.

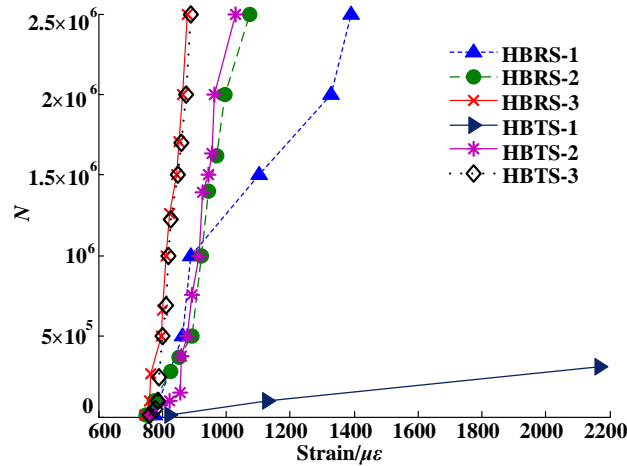


Fig. 7 The number of load cycles  $N$  versus tension HRBF500 bars strains at mid-span

The mean value of the ratio of calculated values according to Eq. (10) to experimental values was 1.0267, and the standard deviation and coefficient of variation were 0.0999 and 0.0973 respectively, which indicated that Eq. (10) can give accurate prediction for mid-span deflection evolution of HRBF500 bars reinforced concrete beams with different steel ratios under constant cyclic loading.

### 3.3 Analysis of tension HRBF500 bars strain.

Fig. 7 presents the change in the strain of tension HRBF500 bars at mid-span under maximum fatigue load with increasing number of load cycles for the specimens. As shown in Fig. 7, the increases in the strain of HRBF500 steel bars were most marked in the early stages of fatigue loading, after which the increasing rate of the strain of HRBF500 steel bars reduced considerably. In addition, there are no significant differences in variation law of tension HRBF500 bars strains for rectangular and T-section beams. The percentage increase in tension HRBF500 bars strain over the initial value for each beam is given in Table 4. As Table 4 shows, except specimen HBTS-1, the bigger the steel ratio was, the smaller the percentage increase of tensile HRBF500 reinforcement strain was. The strain of HRBF500 bars in specimen HBTS-1 increased fastest of all specimens, because the initial tensile stresses of HRBF500 bars in specimen HBTS-1 produced by the upper-bound fatigue loads were biggest.

As discussed above, number of load cycles  $N$ , steel ratio and the initial tensile stresses of HRBF500 bars were the main factors affecting the strain variation of HRBF500 bars. Then the quantitative relationship between the strain increase in HRBF500 bars and number of load cycles  $N$  was analyzed in the stable growth stage (loading cycles  $N$  is not less than 50,000) for the test beams that survived 2.5 million cycles of constant-amplitude cyclic loading, as well as the relationship between the strain of HRBF500 steel bars and steel ratio.

Strain increase coefficient  $\lambda$  was defined as follow

$$\lambda = \varepsilon / \varepsilon_1 - 1 \quad (12)$$

where  $\varepsilon_1$  denotes the initial strain of HRBF500 bars at mid-span corresponding to the maximum

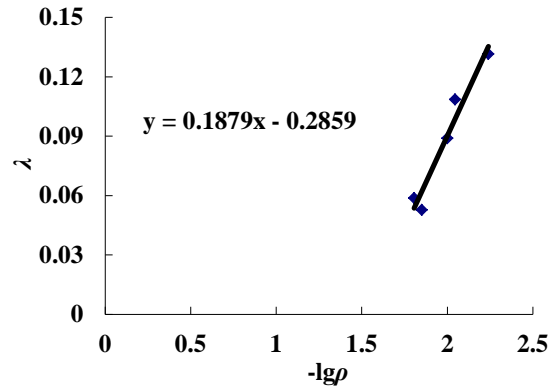


Fig. 8 Strain increase coefficient  $\lambda$  versus tension reinforcement ratio  $\rho$  at 500,000 load cycles

fatigue load, and  $\varepsilon$  represents the strain of HRBF500 bars at mid-span corresponding to the maximum fatigue load at different load cycles during fatigue test.

According to experimental data, the relationship between strain increase coefficient  $\lambda$  and the tension reinforcement ratio  $\rho$  for specimens at 500,000 number of load cycles is shown in Fig. 8. As indicated in Fig. 8, strain increase coefficient  $\lambda$  increased linearly as the logarithm of tension reinforcement ratio  $\rho$  increased. Through linear regression, the relationship between strain increase coefficient  $\lambda$  and tension reinforcement ratio  $\rho$  at 500,000 number of load cycles was obtained as follow

$$\lambda = 0.1879(-\lg \rho) - 0.2859 \quad (13)$$

Similarly, the relationship between strain increase coefficient  $\lambda$  and the tension reinforcement ratio  $\rho$  for specimens at 1 million, 1.5 million, 2 million and 2.5 million number of load cycles were expressed by the equations as follow

$$\text{at 1 million load cycles, } \lambda = 0.3816(-\lg \rho) - 0.5997 \quad (14)$$

$$\text{at 1.5 million load cycles, } \lambda = 0.6879(-\lg \rho) - 1.1290 \quad (15)$$

$$\text{at 2 million load cycles, } \lambda = 1.2353(-\lg \rho) - 2.1344 \quad (16)$$

$$\text{at 2.5 million load cycles, } \lambda = 1.4115(-\lg \rho) - 2.4215 \quad (17)$$

The mean value of the ratio of calculated values according to Eqs. (13)-(17) to experimental values was 1.0003, and the standard deviation and coefficient of variation were 0.021 and 0.021 respectively, which indicated that the calculated values were in good agreement with experimental results. Through analysis of the Eqs. (15)-(19), it can be found that, the relationship between strain increase coefficient  $\lambda$  and tension reinforcement ratio  $\rho$  can be expressed by the equation as follows

$$\lambda = c(-\lg \rho) + d \quad (18)$$

Then the influence of number of load cycles  $N$  in the coefficients  $c$  and  $d$  in Eq. (18) was discussed. By linear regression, the relationship between the values of coefficients  $c$  and  $d$  in Eqs.

(13)-(17) and number of load cycles  $N$  can be expressed as

$$c = 0.0066n - 0.2094 \quad (19)$$

$$d = -0.0116n + 0.4277 \quad (20)$$

Taking Eqs. (12), (19) and (20) into Eq. (18), the strain of tension HRBF500 bars in mid-span under maximum fatigue load can be calculated by the equation as follows

$$\varepsilon = [(0.0066n - 0.2094)(-\lg \rho) - 0.0116n + 1.4277] \varepsilon_1 \quad (21)$$

The mean value of the ratio of calculated values according to Eq. (21) to experimental values was 1.0013, and the standard deviation and coefficient of variation were 0.024 and 0.024 respectively, which indicated that Eq. (21) can accurately predict strain variation of tension HRBF500 bars in concrete beams with different steel ratios under constant fatigue loading.

#### 4. Conclusions

Three rectangular and three T-section RC beams reinforced with HRBF500 steels were constructed and tested under static and fatigue loading. The specimens were designed with different steel ratios. The following conclusions can be drawn based on the static and fatigue tests results presented in this paper:

1. The widths of cracks increased with increasing number of load cycles. The RC beams with HRBF500 bars can withstand 2.5 million cycles of constant-amplitude fatigue loading without apparent signs of damage, if they meet the following requirements: the initial stresses of their HRBF500 tension reinforcements produced by the maximum fatigue load are not more than 150 MPa, and reinforced with appropriate amount of HRBF500 bars.

2. The deflections of test beams increased with increasing number of load cycles. There was pronounced increases in mid-span deflections in the initial 100,000 cycles, after which stable behaviors were observed with only slight increases in mid-span deflections. The bigger the steel ratio was, the smaller the percentage increase in mid-span deflection was.

3. The quantitative relationship between the deflection increase and number of load cycles  $N$  was fully discussed, as well as the relationship between the deflection increase and steel ratio. And the prediction model of mid-span deflection evolution of HRBF500 bars reinforced concrete beams with different steel ratios under constant cyclic loading was obtained.

4. The tensile stresses of HRBF500 steel bar in the test beams grew as the number of fatigue cycles increased. The increases in the strain of HRBF500 steel bars were most marked in the early stages of fatigue loading, after which the increasing rate of the strain of HRBF500 steel bars reduced considerably. The bigger the steel ratio was, the smaller the percentage increase in tensile HRBF500 reinforcement strain was.

5. The quantitative relationship between the tensile strain of HRBF500 steel bars and number of load cycles  $N$  was analyzed, as well as the relationship between the strain of HRBF500 steel bars and steel ratio. And the prediction model of strain variation of tension HRBF500 bars in concrete beams with different steel ratios under constant cyclic loading was obtained.

6. The initial extreme tension steel stress, stress range and steel ratio were the main factors that affected the fatigue properties of RC beams with HRBF500 bars. The bigger the tension reinforcement stress range was, the larger the increase in the tension reinforcement strain and mid-

span deflection of the specimen were. Cross-sectional shape has no significant influence in fatigue properties of RC beams with HRBF500 bars.

## Acknowledgments

The research described in this paper was financially supported by a grant from the Major State Basic Research Development Program of China (973 Program) (No. 2012CB026200) and a grant from the National High Technology R&D Program of China (863 Program) (No. 2008AA030704).

## References

- Al-Hammoud, R., Soudki, K. and Topper, T.H. (2010), "Bond analysis of corroded reinforced concrete beams under monotonic and fatigue loads", *Cement Concrete Compos.*, **32**(3), 194-203.
- Al-Rousan, R. and Issa, M. (2011), "Fatigue performance of reinforced concrete beams strengthened with CFRP sheets", *Construct. Build. Mater.*, **25**(8), 3520-3529.
- Aidoo, J., Harries, K.A. and Petrou, M.F. (2004), "Fatigue behavior of carbon fiber reinforced polymer strengthened reinforced concrete bridge girders", *J. Compos. Constr.*, **8**(6), 501-509.
- Chapetti, M.D., Miyata, H., Tagawa, T., Miyata, T. and Fujioka, M. (2004), "Fatigue strength of ultra-fine grained steels", *Mater. Sci. Eng.: A*, **381**(1-2), 331-336.
- Chapetti, M.D., Miyata, H., Tagawa, T., Miyata, T. and Fujioka, M. (2005), "Fatigue crack propagation behaviour in ultra-fine grained low carbon steel", *Int. J. Fatig.*, **27**(3), 235-243.
- El-Tawil, S., Ogunc, C., Okeil, A. and Shahawy, M. (2000), "Static and fatigue analyses of RC beams strengthened with CFRP laminates", *J. Compos. Constr.*, **5**(4), 258-267.
- Grace, N.F. and Ross, B. (1996), "Dynamic characteristics of post-tensioned girders with web openings", *J. Struct. Eng.*, **122**(6), 643-650.
- Harajli, M.H. and Namaan, A.E. (1985), "Static and fatigue test on partially prestressed beam", *J. Struct. Eng.*, **111**(7), 1608-1618.
- Heffernan, P.J. and Erki, M.A. (2004), "Fatigue behavior of reinforced concrete beams strengthened with carbon fiber reinforced plastic laminates", *J. Compos. Constr.*, **8**(2), 132-140.
- Kennedy, J.B., Chami, S. and Grace, N.F. (1990), "Dynamic and fatigue responses of prestressed concrete girders with openings", *Can. J. Civil Eng.*, **17**(3), 460-470.
- Kim, H.K., Choi, M.I., Chung, C.S. and Shin, D.H. (2003), "Fatigue properties of ultrafine grained low carbon steel produced by equal channel angular pressing", *Mater. Sci. Eng.: A*, **340**(1-2), 243-250.
- Kim, Y.J. and Harries, K.A. (2011), "Fatigue behavior of damaged steel beams repaired with CFRP strips", *Eng. Struct.*, **33**(5), 1491-1502.
- Kormeling, H.A., Reinhardt, H.W. and Shah, S.P. (1980), "Static and fatigue properties of concrete beams reinforced with continuous bars and with fibers", *J. Am. Concrete Ins.*, **77**(1), 36-43.
- Mughrabi, H. and Höppel, H.W. (2010), "Cyclic deformation and fatigue properties of very fine-grained metals and alloys", *Int. J. Fatig.*, **32**(9), 1413-1427.
- Muller, J.F. and Dux, P.F. (1994), "Fatigue of prestressed concrete beams with inclined strands", *J. Struct. Eng.*, **120**(4), 1122-1139.
- Okayasu, M., Sato, K., Mizuno, M., Hwang, D.Y. and Shin, D.H. (2008), "Fatigue properties of ultra-fine grained dual phase ferrite/martensite low carbon steel", *Int. J. Fatig.*, **30**(8), 1358-1365.
- Park, K.T., Kim, Y.S., Lee, J.G. and Shin, D.H. (2000), "Thermal stability and mechanical properties of ultrafine grained low carbon steel", *Mater. Sci. Eng.: A*, **293**(1-2), 165-172.
- Patlan, V., Vinogradov, A., Higashi, K. and Kitagawa, K. (2001), "Overview of fatigue properties of fine grain 5056 Al-Mg alloy processed by equal-channel angular pressing", *Mater. Sci. Eng.: A*, **300**(1-2), 171-

182.

Roller, J.J., Russell, H.G. and Bruce, R.N. (2007), "Fatigue endurance of high-Strength prestressed concrete bulb-tee girders", *PCI J.*, **52**(3), 30-42.

Shahawi, M.E. and Batchelor, B.D. (1986), "Fatigue of partially prestressed concrete", *J. Struct. Eng.*, **112**(3), 524-537.

Shahawy, M. and Beitelman, T.E. (1999), "Static and fatigue performance of RC beams strengthened with CFRP laminates", *J. Struct. Eng.*, **125**(6), 613-621.

Takaki, S., Kawasaki, K. and Kimura, Y. (2001), "Mechanical properties of ultra fine grained steels", *J. Mater. Pr. Tech.*, **117**(3), 359-363.

Thandavamoorthy, T.S. (1999), "Static and fatigue of high-ductility bars reinforced concrete beams", *J. Mater. Civil Eng.*, **11**(1), 41-50.

CC